Proceedings of the Estonian Academy of Sciences,
2019, **68**, 2, 150–157
https://doi.org/10.3176/proc.2019.2.06
Available online at www.eap.ee/proceedings

MATERIALS
ENGINEERING

Study of submerged and plasma arc welded composite hardfacings with a novel Cr_3C_2–Ni reinforcement

Regita Bendikiene[a*], Antanas Ciuplys[a], Simonas Mindaugas Jankus[a], Andrei Surzhenkov[b*], Dmytro Tkachivskyi[b], Kristjan Juhani[b], Mart Viljus[b], Rainer Traksmaa[b], Maksim Antonov[b], and Priit Kulu[b]

[a] Department of Production Engineering, Faculty of Mechanical Engineering and Design, Kaunas University of Technology, Studentu gatve 56, 51424 Kaunas, Lithuania
[b] Department of Mechanical and Industrial Engineering, Tallinn University of Technology, Ehitajate tee 5, 19086 Tallinn, Estonia

Received 31 January 2019, accepted 12 March 2019, available online 13 May 2019

Abstract. This paper studies possible uses of Cr_3C_2–Ni cermet prepared via mechanically activated synthesis as reinforcement in submerged arc welded (SAW) and plasma transferred arc welded (PTAW) Fe- and Ni-based hardfacings. The microstructure and phase composition of the hardfacings were analysed by scanning electron microscopy and X-ray diffraction, respectively. Vickers hardness (HV30) was measured and two-body (ASTM G132) and three-body (ASTM G65) abrasive wear were tested. Cermet particles were found to be entirely dissolved in the SAW hardfacings, while in the PTAW hardfacings they were partially retained. The main phases in the Fe-based hardfacings were γ-Fe and α-Fe along with Cr_7C_3 in the PTAW hardfacing. The Ni-based SAW and PTAW hardfacings were mostly comprised of different carbides (Cr_3C_2, CrC, $NiC_{0.22}$). Addition of cermet particles increased the hardness of the hardfacings 1.1–3.3 times, the effect being more pronounced in the Fe-based hardfacings and PTAW hardfacings. Under two-body abrasive wear conditions, composite hardfacings exhibited 1.2–7.8 times lower wear and under three-body abrasive wear conditions 1.4–9.4 times lower wear than the unreinforced hardfacings. The wear resistance of the PTAW hardfacings was improved considerably, while the effect of the matrix alloy was insignificant. Microcutting was the major wear mechanism under both two-body and three-body abrasive wear conditions, accompanied by microploughing in the SAW hardfacings in the former case and by the pull-out of carbide particles in the PTAW hardfacings in the latter case. The principle of the wear mechanism remained unaltered in the presence of cermet particles, but the wear was less severe.

Key words: composite hardfacing, cermet reinforcement, submerged arc welding, plasma transferred arc welding, abrasive wear.

1. INTRODUCTION

Despite their obvious advantages, for example high hardness and high melting point, the most frequently used reinforcements in cladded composite hardfacings such as tungsten carbide (WC) [1–4] and WC-based hardmetals [5–7], as well as titanium carbide [2,8–10] exhibit certain limitations. For example, WC and WC-based hardmetals are prone to degradation above 500 °C with the formation of a brittle WO_3 layer [11,12]. The price of both tungsten and cobalt has fluctuated to a large extent over decades; moreover, cobalt has been classified as a toxic metal [13]. As to TiC, several authors have reported its uneven distribution in a hardfacing [8,9] due to different densities of the molten metal matrix and titanium carbide [14], which may deteriorate the mechanical properties of the hard-

* Corresponding authors, andrei.surzenkov@taltech.ee, regita.bendikiene@ktu.lt

facing [9]. Therefore, alternative reinforcement materials are required.

Relatively few studies have focused on separately synthesized chromium carbide (Cr_3C_2) or a Cr_3C_2-based cermet as reinforcement candidates and on their influence on the wear resistance of hardfacings. Nurminen et al. [2] found that despite a high dissolution rate of Cr_3C_2 in the Ni-based alloy, the Cr_3C_2 reinforced hardfacing exhibits the lowest wear among the studied Ni- and Co-based hardfacings reinforced with tungsten, chromium, and vanadium carbides. According to Goswami et al. [15], addition of chromium carbide to a Ni–Cr alloy hardfacing reduces its wear rate remarkably as compared to the analogous hardfacing from the Stellite 6 alloy. In [16–18] it was shown that addition of approximately 30 wt% Cr_3C_2 particles to a Ni-based alloy improves their wear resistance by 1.5–1.7 times. Luo et al. [19] reported that the relative abrasive wear resistance of a chromium carbide reinforced Ni_3Al hardfacing is up to six times higher than that of the Stellite 12 alloy. Janicki [20] obtained up to three times higher erosion wear resistance with the introduction of porous chromium carbide to the nickel-based laser-clad matrix. Zikin et al. [11] demonstrated that Cr_3C_2-based cermet reinforcement is more favourable than Cr_3C_2 due to its lower dissolution rate.

One of the obstacles associated with the application of carbide-based cermets in hardfacings is their relatively high price [21]. One of the ways to lower it is to synthesize the carbide phase in situ during the sintering process [22–24]. To raise the reactivity of the feedstock powders, several researchers have proposed mechanical activation by high-energy ball milling [23,25,26]. The production of Cr_3C_2-based powders for thermal spraying by such a technology was recently reported in [21,27]; however, their perspective as a reinforcement phase in cladded hardfacings is still unclear.

The present research concentrates on the Ni- and Fe-based composite hardfacings with a novel Cr_3C_2–Ni cermet reinforcement. The influence of the cladding technology and of the matrix alloy on the microstructure, hardness, and two- and three-body abrasive wear is studied.

2. EXPERIMENTAL

2.1. Preparation of the reinforcement

Mechanically activated synthesis (MAS) of Cr_3C_2–Ni powder reinforcement described in detail in [21] was used. To obtain the Cr_3C_2–Ni (80 wt% Cr_3C_2, 20 wt% Ni) cermet powder, powders of pure Cr (99.5 wt%; average particle size 6.65 μm) and pure Ni (99.7 wt%; average particle size 2.4 μm), supplied by Pacific Particulate Materials Ltd., as well as pure carbon black (99.7 wt%; average particle size 6.45 μm), supplied by Imerys SA, were milled in the conventional ball mill with hardmetal balls (ball-to-powder ratio 20 : 1) in isopropanol during 72 h, then plasticized and sintered in vacuum at 1100 °C to obtain bulk compacts. The sintered agglomerates were manually crushed and the powder fraction suitable as reinforcement (size range 90–300 μm) was sieved.

2.2. Deposition of hardfacings

Two deposition technologies – submerged arc welding (SAW) and plasma transferred arc welding (PTAW) – were used to prepare the hardfacings. The deposition parameters are provided in Table 1. For SAW, the consumable Ø1.2 mm wire electrode (wt%: 0.1 C, <0.03 Si, 0.35–0.6 Mn, <0.15 Cr, <0.3 Ni, bal. Fe) and flux ОЦК-45 (wt%: 38–44 SiO_2, 38–44 MnO, <2.5 MgO, 6–9 CaF_2, <6.5 CaO, <2 Fe_2O_3, <0.15 S, < 0.15 P) were applied. For PTAW, the Ø3.2 mm non-consumable bulk electrode WT 20 (wt%: 98.0 W, 2.0 ThO_2) was used. The normalized structural steel S355 (wt%: 0.22 C, 1.60 Mn, 0.05 Si, 0.05 P, 0.05 S, bal. Fe) was used as the substrate steel in all the cases. Table 2 shows the designation and the chemical composition of the hardfacings. In the composite hardfacings, the rate of the matrix and reinforcement in the hardfacings was adjusted to be 60 : 40 wt%. Prior to the PTAW process, the

Table 1. Deposition equipment and parameters

Process	Equipment (manufacturer)	Current, A	Voltage, V	Oscillation frequency, Hz	Traverse speed, mm/s	Gas consumption, L/s
SAW	Integra 350 Professional (Miller)	180	22–24	–	4	–
PTAW	GAP 3001 DC (Castolin Eutectic®)	95	22–24	0.6	1	Plasma gas (Ar) – 1.5 Shield gas (Ar) – 6.5 Carrier gas (Varigon®*) – 3.75 (reinforcement), 2.75 (matrix)

* 95% Ar + 5% H_2.

Table 2. Designation and chemical composition of the hardfacings

Designation	Deposition technology	Matrix composition, wt%	Reinforcement composition
SAW-SS	SAW	99.9 stainless steel* + 0.1 wire electrode	–
SAW-Ni	SAW	99.9 Ni alloy** + 0.1 wire electrode	–
SAW-SS+CrC	SAW	99.9 stainless steel + 0.1 wire electrode	Cr_3C_2–Ni***
SAW-Ni+CrC	SAW	99.9 Ni alloy + 0.1 wire electrode	Cr_3C_2–Ni
PTAW-SS	PTAW	Stainless steel	–
PTAW-Ni	PTAW	Ni alloy	–
PTAW-SS+CrC	PTAW	Stainless steel	Cr_3C_2–Ni
PTAW-Ni-CrC	PTAW	Ni alloy	Cr_3C_2–Ni

* Austenitic stainless steel EN-X3CrNiMo17-13-3; powder grade Castolin 16316 (wt%: 0.03 C, 17.5 Cr, 13 Ni, 2.7 Mo, bal. Fe).
** Ni-based self-fluxing alloy; powder grade Castolin 16221 (wt%: 0.2 C, 4 Cr, 1 B, 2.5 Si, max. 2 Fe, 1 Al, bal. Ni).
*** Experimental cermet powder, produced by the MAS route.

powders were dried at 50 °C for 5 h, while no drying of powders was applied in the SAW process.

2.3. Microstructure studies

The microstructure of the obtained hardfacings was studied using a scanning electron microscope (SEM) EVO MA-15 (Carl Zeiss, Germany), equipped with an energy dispersive spectroscopy (EDS) device. An X-ray diffraction (XRD) device AXS D5005 (Bruker, Germany), equipped with a Cu Kα radiation source, was used to study the phase composition of the hardfacings (measuring step 0.04°).

2.4. Hardness measurements

Vickers surface hardness (HV30) of the surface of the hardfacings was measured by using the Vickers hardness tester Indentec 5030KV (Zwick/Roell, Germany) at the load 294.3 N (30 kgf) and the dwell time 10 s. Ten measurements were made at each hardfacing, and the average hardness value was calculated.

2.5. Wear tests

The data on the applied wear tests are given in Table 3. The size of the tested specimens was 6 mm × 20 mm × 10 mm and 50 mm × 25 mm × 10 mm for the two-body and three-body wear tests, respectively. Three specimens of each hardfacing type were tested, and the average volumetric wear was determined. Worn surfaces of the hardfacings were studied with SEM EVO MA-15 (Carl Zeiss) and FEI Quantra FEG (Bruker Quantax) to find out the wear mechanisms.

3. RESULTS AND DISCUSSION

3.1. Microstructure analysis

Unreinforced hardfacings had microstructures, typical for welded Fe- and Ni-based hardfacings reported elsewhere [7,11]. Therefore, they are not analysed here. Particles of the Cr_3C_2–Ni reinforcement were entirely dissolved in the SAW hardfacings (Fig. 1a,c), while in the PTAW hardfacings, cermet particles remained integral (Fig. 1b,d). The reason was most probably the higher welding current during the SAW process, which according to the Joule–Lenz law, would lead to a higher heat input to the hardfacing and, consequently, to a higher dissolution rate. Apart from that, the amount of the retained Cr_3C_2–Ni reinforcement was much lower in the Fe-based hardfacing, which is intrinsic to the Fe-based hardfacings [2].

Table 3. Parameters of the wear tests

Test type	Standard designation	Force, N	Speed of rotation, L/s	Linear speed, m/s	Duration, s	Abrasive type	Abrasive size, mm	Other parameters
Two-body	ASTM G132	5	1.05	0.4	3600	Al_2O_3	0.08–0.1	Emery paper was changed after each 300 s
Three-body	ASTM G65, procedure A	130	3.6	2.4	1800	SiO_2	0.2–0.3	Abrasive mass flow rate $(5.0–6.7) \times 10^{-2}$ kg/s

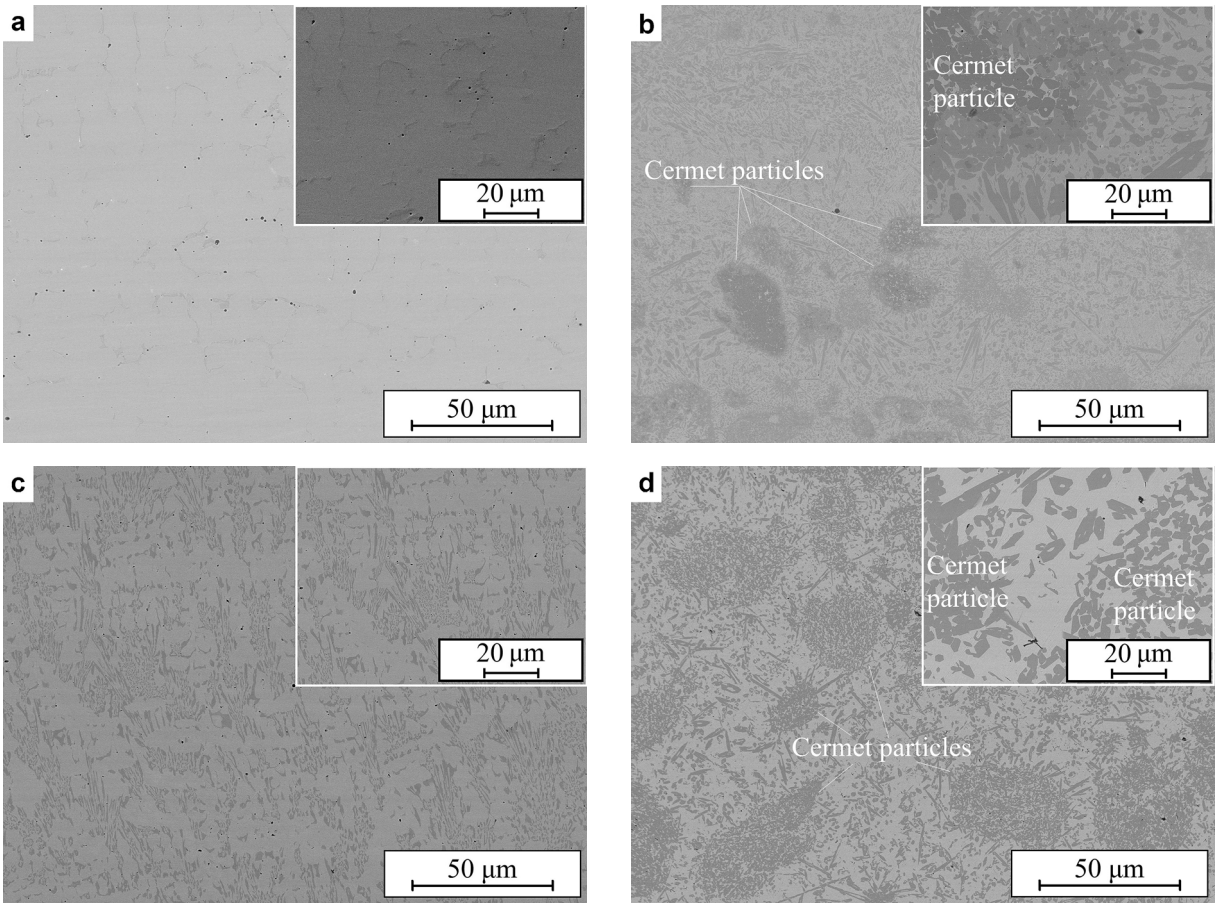

Fig. 1. Microstructure of the hardfacings: a – SAW-SS+CrC, b – PTAW-SS+CrC, c – SAW-Ni+CrC, d – PTAW-Ni+CrC.

3.2. Phase composition

Almost no differences were found between the unreinforced Fe- and Ni-based SAW and PTAW hardfacings. For this reason, the phase composition of these hardfacings is not analysed here. The principal phases in the SAW-SS+CrC hardfacing were solid solution of Cr in α-Fe and, on a smaller scale, Ni-rich retained austenite (γ-Fe) and a small amount of secondary carbide Cr_3C, while Cr_7C_3 and austenite (γ-Fe) prevailed in the microstructure of the PTAW-SS+CrC hardfacing accompanied by the solid solution of Fe(Cr) (Fig. 2a). The relatively small amount of secondary carbides could be explained by the dissolution of carbon in the retained austenite.

The SAW-Ni+CrC hardfacing comprised mostly different chromium carbides (CrC, Cr_3C_2) and, on a minor scale, γ-Fe (Fig. 2b). The PTAW Ni+CrC hardfacing contained mostly primary Cr_3C_2 carbide and nickel-based secondary carbide $NiC_{0.22}$, accompanied by minor amounts of Cr_3Si and Cr_2B (not indicated in the XRD chart).

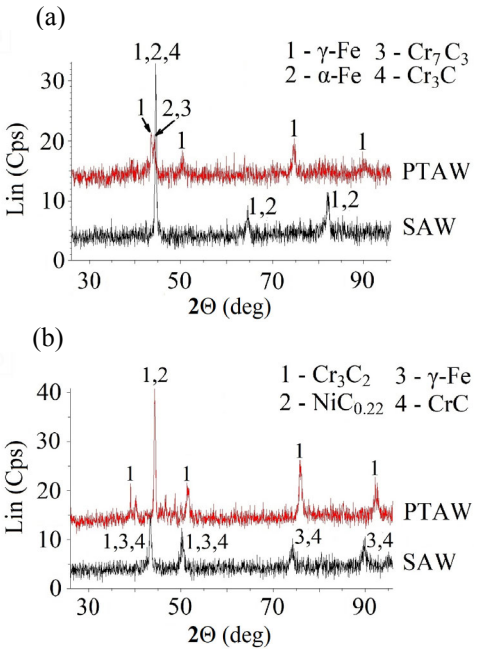

Fig. 2. XRD charts of the hardfacings: a – SS-type hardfacings, b – Ni-type hardfacings.

3.3. Hardness studies

Addition of Cr_3C_2–Ni particles increased the average hardness of the hardfacings by 1.1–3.3 times. A larger growth was observed in the case of the stainless steel matrix hardfacings and PTAW hardfacings (Fig. 3). The latter may be explained by the presence of retained cermet particles in the matrix. A larger increase of the hardness of SS-CrC type hardfacings is the result of the relatively low initial hardness of unreinforced hardfacings made of stainless steel.

3.4. Wear of the hardfacings

The results of the wear tests generally correlated with those of hardness. Under the two-body abrasive wear conditions, the composite SAW hardfacings exhibited 1.2–1.8 times lower wear, and composite PTAW hardfacings, 6.7–7.8 times lower wear than the respective unreinforced hardfacings (Fig. 4). Analogously, under the three-body abrasion wear conditions addition of Cr_3C_2–Ni particles to the Ni- or Fe-based alloy led to 1.4–1.8 times lower wear of the SAW hardfacings and 9.2–9.4 times lower wear of the PTAW hardfacings (Fig. 5).

The increase of wear resistance was more pronounced in the case of Fe-based hardfacings and PTAW hardfacings. A larger enhancement of the wear resistance of the latter may be explained by the retention of Cr_3C_2–Ni particles in the hardfacings. The relatively lower wear of the SS-CrC type hardfacings, stress-induced martensitic transformation of the retained austenite, which happens during the wear test [28], may be suggested as the most probable cause.

As the SS-CrC type hardfacings exhibited the lowest overall wear, they were used in the analysis of the wear mechanisms (Fig. 6). Under the two-body abrasive wear, the wear mechanism of the SAW hardfacing was a combination of microcutting and microploughing (Fig. 6a). In the case of the PTAW hardfacing, microcutting became dominant and the grooves left by abrasive particles became shallower (Fig. 6b). Material loss due to the spalling of flat fragments became insignificant as well. A better wear resistance of the PTAW SS-CrC hardfacings may be explained by a larger amount of primary as well as secondary carbides. Under the three-body abrasive wear conditions, microcutting was the common wear mechanism of both the SAW (Fig. 6c) and the PTAW hardfacing (Fig. 6d). However, the depth and the length of the grooves were obviously larger in the SAW hardfacing, as cermet reinforcement tackled the movement of free abrasive and its penetration inside the matrix in the PTAW hardfacing. Loss of carbide particles from the cermet reinforcement was also observed, although the cermet particles themselves remained holistic, which is a sign of their good integration with the matrix.

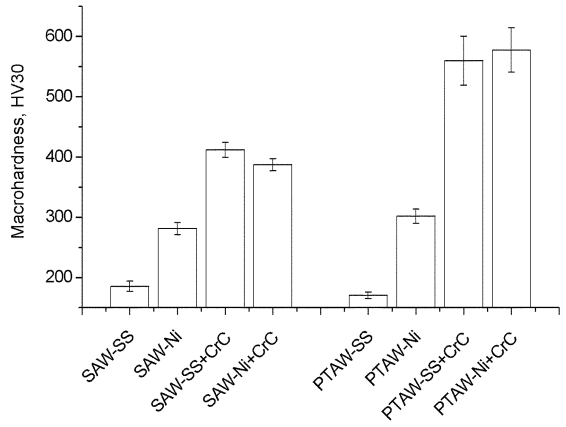

Fig. 3. Vickers macrohardness of the hardfacings.

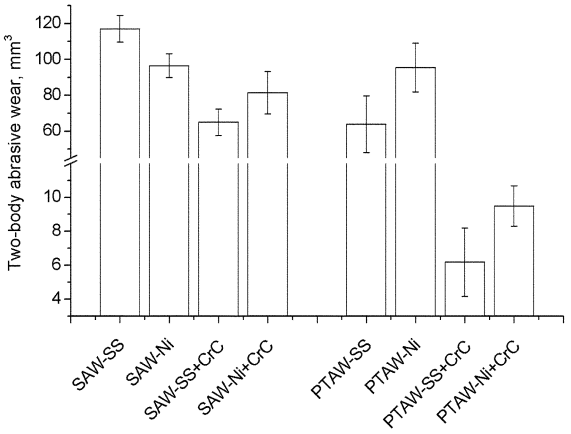

Fig. 4. Two-body abrasive wear of hardfacings.

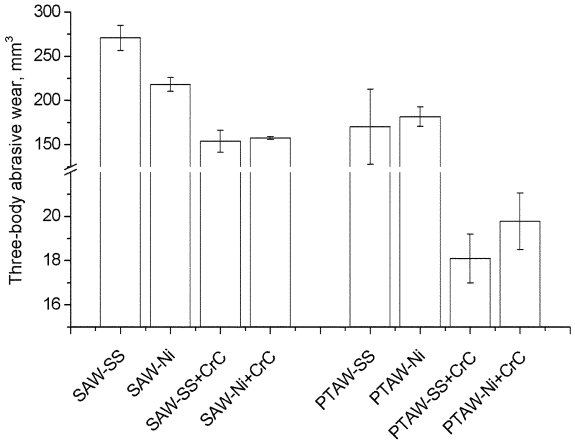

Fig. 5. Three-body abrasive wear of hardfacings.

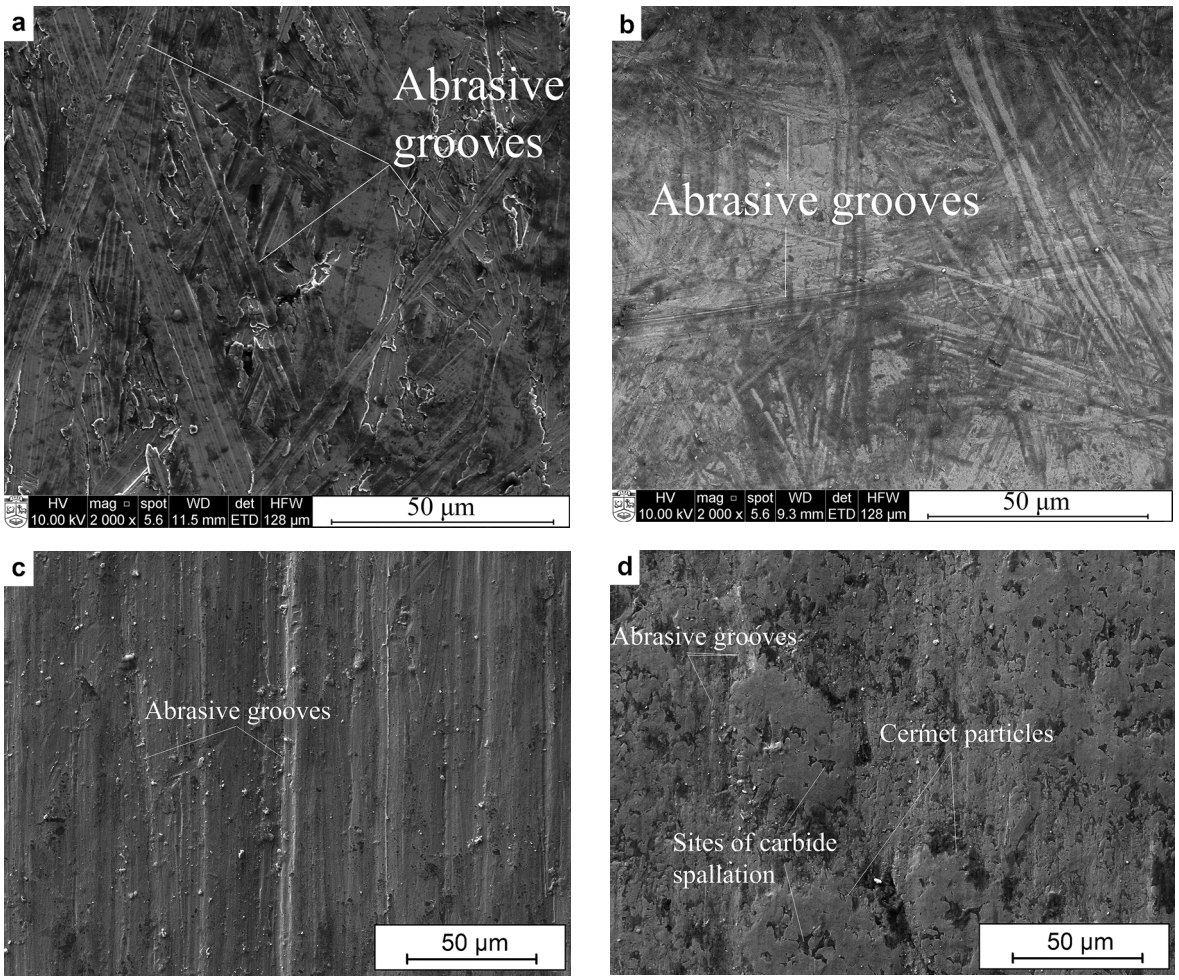

Fig. 6. Worn surfaces of the hardfacings: a – SAW SS-CrC, two-body abrasive wear; b – PTAW SS-CrC, two-body abrasive wear; c – SAW SS-CrC, three-body abrasive wear; d – PTAW SS-CrC three-body abrasive wear.

4. CONCLUSIONS

- It is possible to efficiently use Cr_3C_2–Ni cermet produced by mechanically activated synthesis (MAS) as a reinforcement in composite welded hardfacings, although it is more feasible in the plasma transferred arc welding (PTAW) process than in the submerged arc welding (SAW) process.
- The dissolution rate of Cr_3C_2–Ni particles was higher in the Fe-based hardfacing than in the Ni-based one, and the re-precipitation rate of secondary carbides was the lowest in the Fe-based SAW hardfacing.
- Reinforcement by Cr_3C_2–Ni cermet particles led to 1.1–3.3 times higher hardness as compared with the unreinforced coating; this effect was more pronounced in the case of PTAW hardfacings and hardfacings with a Fe-based matrix.
- Addition of Cr_3C_2–Ni cermet particles improved the wear resistance of the hardfacings both under two- and three-body abrasive wear conditions by 1.2–9.4 times; this effect was greater in the case of PTAW hardfacings, as well as under the three-body abrasive wear conditions, while the influence of the matrix alloy was insignificant.
- Retention of primary Cr_3C_2–Ni particles led to the formation of a harder and stronger structure, which was more resistant to wear.

ACKNOWLEDGEMENTS

This work was supported by institutional research funding IUT19-29 ‘Multi-scale structured ceramic based composites for extreme applications’ of the Estonian Ministry of Education and Research and by project B56 ‘Innovative polycrystalline diamond (PDC) drag bit for soft ground tunnel boring machines’. This research was also partially supported by the Graduate School of Functional Materials and Technologies (project No. 2014-2020.4.01.16-0027), receiving funding from the European Regional Development Fund in the University of Tartu, Estonia.The publication costs of this article were covered by the Estonian Academy of Sciences.

REFERENCES

1. Gassmann, R. C. Laser cladding with (WC+W_2C)/Co–Cr–C and (WC+W_2C)/Ni–B–Si composites for enhanced abrasive wear resistance. *Mater. Sci. Technol*, 1996, **12**, 691–696.
2. Nurminen, J., Näkki, J., and Vuoristo, P. Microstructure and properties of hard and wear resistant MMC coatings deposited by laser cladding. *Int. J. Refract. Met. H. Mater*., 2009, **27**, 472–478.
3. Surzhenkov, A., Baroninš, J., Viljus, M., Traksmaa, R., and Kulu, P. Sliding wear of composite stainless steel hardfacing under room and elevated temperature. *Sol. St. Phen.*, 2017, **267**, 195–200.
4. Sui, Y., Yang, F., Qin, G., Ao, Z., Liu, Y., and Wang, Y. Microstructure and wear resistance of laser-cladded Ni-based composite coatings on downhole tools. *J. Mater. Process. Technol*, 2018, **252**, 217–224.
5. Wang, P-Z., Qu, J-X., and Shao, H-S. Cemented carbide reinforced nickel-based alloy coating by laser cladding and the wear characteristics. *Mater. Design*, 1996, **17**, 289–296.
6. Bendikiene, R., Ciuplys, A., and Kavaliauskiene, L. Preparation and wear behaviour of steel turning tools surfaced using the submerged arc welding technique. *Proc. Estonian Acad. Sci.*, 2016, **65**, 117–122.
7. Bendikiene, R., Ciuplys, A., and Pupelis, E. Research on possibilities to replace industrial wear plates by surfaced coatings using waste materials. *Int. J. Surf. Sci. Eng.*, 2016, **10**, 330–338.
8. Liu, J., Wang, L., and Li, H. Reactive plasma cladding of TiC/Fe cermet coating using asphalt as a carbonaceous precursor. *Appl. Surf. Sci.*, 2009, **255**, 4921–4925.
9. Emamian, A., Alimardani, M., and Khajepour, A. Correlation between temperature distribution and in situ formed microstructure of Fe–TiC deposited on carbon steel using laser cladding. *Appl. Surf. Sci.*, 2012, **258**, 9025–9031.
10. Sahoo, C. K. and Masanta, M. Microstructure and mechanical properties of TiC-Ni coating on AISI304 steel produced by TIG cladding process. *J. Mater. Process. Technol.*, 2017, **240**, 126–137.
11. Zikin, A., Hussainova, I., Katsich, C., Badisch, E., and Tomastik, C. Advanced chromium carbide-based hardfacings. *Surf. Coat. Technol.*, 2012, **206**, 4270–4278.
12. Humphry-Baker, S. A. and Lee, W. E. Tungsten carbide is more oxidation resistant than tungsten when processed to full density. *Scr. Mater.*, 2016, **116**, 67–70.
13. Kolnes, M. *Cobalt- and Nickel-free Titanium and Chromium Carbide-based Cermets*. PhD thesis. TTÜ Press, Tallinn, 2018.
14. Pelletier, J. M., Jobez, S., Saif, Q., Kirat, P., and Vannes, A. B. Laser surface alloying: mechanism of formation and improvement of surface properties. *J. Mater. Eng.*, 1991, **13**, 281–290.
15. Goswami, G. L., Kumar, S., Galun, R., and Mordike, B. L. Laser cladding of nickel based carbide dispersion alloys for hardfacing applications. *Laser. Eng.*, 2003, **13**, 35–44.
16. Huang, Z., Hou, Q., and Wang, P. Microstructure and properties of Cr_3C_2-modified nickel-based alloy coating deposited by plasma transferred arc process. *Surf. Coat. Tech.*, 2008, **202**, 2993–2999.
17. Zhang, D-W., Lei, T. C., and Li, F-J. Laser cladding of stainless steel with Ni–Cr_3C_2 for improved wear performance. *Wear*, 2001, **251**, 1372–1376.
18. Verdi, D., Garrido, M. A., Munez, C. J., and Poza, P. Cr_3C_2 incorporation into an Inconel 625 laser cladded coating: effects on matrix microstructure, mechanical properties and local scratch resistance. *Mater. Design*, 2015, **67**, 20–27.
19. Luo, H-L., Gong, K., Li, S-P., Cao, X., Zhang, X-C., Feng, D., and Li, C-H. Abrasive wear comparison of Cr_3C_2/Ni_3Al composite and Stellite 12 alloy cladding. *J. Iron Steel Res. Int.*, 2007, **14**(4), 15–20.
20. Janicki, D. Laser cladding of Inconel 625-based composite coatings reinforced by porous chromium carbide particles. *Opt. Laser Technol.*, 2017, **94**, 6–14.
21. Sarjas, H., Juhani, K., Viljus, M., Matikainen, V., and Vuoristo, P. Wear resistance of HVOF sprayed from mechanically activated thermally synthesized Cr_3C_2–Ni powder. *Proc. Estonian Acad. Sci.*, 2016, **65**, 101–106.
22. Wei, C., Song, X., Zhao, S., Zhang, L., and Liu, W. In-situ synthesis of WC–Co composite powder and densification by sinter-HIP. *Int. J. Refract. Met. H.*, 2010, **28**, 567–571.
23. Jõeleht, M., Pirso, J., Juhani, K., Viljus, M., and Traksmaa, R. The formation of reaction sintered (Ti, Mo)C–Ni cermet from nanocrystalline powders. *Int. J. Refract. Met. H.*, 2014, **43**, 284–290.
24. Zhou, W., Zheng, Y., Zhao, Y., Zhang, G., Dong, Z., and Xiong, W. Fabrication of Ti(C,N)-based cermets by in-situ carbothermal reduction of MoO_3 and subsequent liquid sintering. *J. Am. Ceram. Soc.*, 2017, **100**, 1578–1587.
25. Ren, R., Yang, Z., and Shaw, L. L. A novel process for synthesizing nanostructured carbides: mechanically activated synthesis. In *22nd Annual Conference on Composites, Advanced Ceramics, Materials, and Structures: B: Ceramic Engineering and Science Proceedings* (Bray, D., ed.). John Wiley & Sons, Inc., Hoboken, New York, 1998, 461–468.
26. Chicardi, E., Gotor, F. J., Medri, V., Guicciardi, S., Lascano, S., and Córdoba, J. M. Hot-pressing of (Ti, Mt)(C, N)–Co–Mo_2C (Mt = Ta, Nb) powdered cermets synthesized by a mechanically induced self-sustaining reaction. *Chem. Eng. J.*, 2016, **292**, 51–61.
27. Sarjas, H., Surzhenkov, A., Juhani, K., Antonov, M., Adoberg, E., Kulu, P., et al. Abrasive-erosive wear of thermally sprayed coatings from experimental and commercial Cr_3C_2-based powders. *J. Therm. Spray Technol.*, 2017, **26**, 2020–2029.
28. Colaço, R. and Vilar, R. On the influence of the retained austenite in the abrasive wear behaviour of a laser surface melted tool steel. *Wear*, 2005, **258**, 225–231.

Uudse Cr_3C_2–Ni armatuuriga räbustikaar- ja plasmakaarpealekeevitatud komposiitkõvapinnete uuring

Regita Bendikiene, Antanas Ciuplys, Simonas Mindaugas Jankus, Andrei Surzhenkov, Dmytro Tkachivskyi, Kristjan Juhani, Mart Viljus, Rainer Traksmaa, Maksim Antonov ja Priit Kulu

On uuritud mehaaniliselt aktiveeritud termosünteesi abil saadud Cr_3C_2–Ni kermise kasutamise võimalikkust armatuurina räbustikaar- (SAW) ja plasmakaarpealekeevitatud (PTAW) raud- ning nikkelmaatriksiga kõvapinnetes. Mikrostruktuuriuuringud näitasid, et kõvafaasi osakesed olid täielikult lahustunud SAW-pinnetes, kuid osaliselt säilinud PTAW-pinnetes. Põhilised faasid olid γ-Fe ja α-Fe koos Cr_7C_3-ga (PTAW-pinne) raudmaatriksiga pinnetes ning Cr_3C_2, CrC ja $NiC_{0,22}$ nikkelmaatriksiga pinnetes. Kermise kõvafaasina lisamine suurendas pinde kõvadust 1,1–3,3 korda, seejuures kõvaduse tõus oli suurim raudmaatriksiga PTAW-pinde korral. Fikseeritud abrasiiviga abrasiivkulumise tingimustes näitasid komposiitpinded armeerimata pinnetega võrreldes 1,2–7,8 korda paremat kulumiskindlust, fikseerimata abrasiiviga abrasiivkulumise tingimustes 1,4–9,4 korda paremat kulumiskindlust. PTAW-pinnete kulumiskindlus paranes rohkem, kusjuures erineva maatriksi mõju oli vähe märgatav. Kulumismehhanismidest oli mikrolõikamine põhiline kulumismehhanism mõlemat tüüpi abrasiivkulumise tingimustes, sellele lisandus mikrovagude teke ja karbiidiosakeste väljarebimine uuritud pinnetes. Kermiseosakeste lisamine ei muutnud oluliselt kulumismehhanisme.